frontiers | Frontiers in Physics

TYPE Original Research
PUBLISHED 11 November 2024
DOI 10.3389/fphy.2024.1428608

OPEN ACCESS

EDITED BY
Krishnamurthy Manchikanti,
Tata Institute of Fundamental Research, India

REVIEWED BY
Prashant Kumar Singh,
Tata Institute of Fundamental Research (Hyderabad), India
Dong Wu,
Shanghai Jiao Tong University, China

*CORRESPONDENCE
N. Nissim,
noaznissim@gmail.com

RECEIVED 06 May 2024
ACCEPTED 15 October 2024
PUBLISHED 11 November 2024

CITATION
Nissim N, Henis Z, Eliezer S, Schweitzer Y, Daponta C and Moustaizis S (2024) Boosting of fusion reactions initiated by laser accelerated proton beam in a non-thermal neutral and non-neutral proton-boron plasma.
Front. Phys. 12:1428608.
doi: 10.3389/fphy.2024.1428608

Boosting of fusion reactions initiated by laser accelerated proton beam in a non-thermal neutral and non-neutral proton-boron plasma

N. Nissim[1]*, Z. Henis[1], S. Eliezer[1], Y. Schweitzer[1], C. Daponta[2] and S. Moustaizis[2]

[1]Applied Physics Department, Soreq Nuclear Research Center, Yavne, Israel, [2]Lab of Matter Structure and Laser Physics, Technical University of Crete, Chania, Greece

In this paper we explore the possibility of boosting the reactivity of non-thermal proton-boron fusion triggered by an external proton beam in a plasma at densities near and lower than solid density and temperature characteristic to laser plasma interaction. Suprathermal protons generated by collisions with alpha particles, as well as energetic protons created by the beam protons that do not undergo fusion during the stopping down in the bulk plasma, are accounted for. In addition, we conduct calculations for non-neutral plasma, motivated by recent suggestion that the number of fusion events in such system may be increased.

KEYWORDS

proton boron fusion, stopping power, plasma, avalanche, beam

1 Introduction

During the last decades there has been renewed interest in proton - boron fusion, triggered by increasing yields of alpha particles in experiments with laser generated proton beams. Proton–boron fusion in the thermonuclear regime is prohibitive due to the low reactivity of pB^{11} fuel at temperatures lower than 100 keV and large bremsstrahlung radiation losses at higher temperatures. High intense laser pulses create non-thermal conditions and enable acceleration of ions to many MeV energies, opening the possibility to obtain nuclear fusion at temperatures of several and up to a few tens of keV. Non-thermal fusion was demonstrated experimentally in several configurations, based on high intensity short pulse lasers. “In-target” configuration, is realized by direct irradiation of solid targets containing hydrogen and boron [1–4]. In the “pitcher-catcher” scheme, protons are accelerated at the rear side of a thin foil target, the “pitcher”, through the mechanism of TNSA (target normal sheath acceleration [5]) and irradiate a solid boron-nitride target, the “catcher” [3, 6–8]. The “pitcher-catcher” scheme resembles traditional beam fusion, triggered by energetic protons generated in particle accelerators. However, the energy spectrum of protons accelerated through the TNSA mechanism is wider than the energy spectrum of accelerator-based protons. Recently, a high yield of alpha particles was measured in experiments with cellulite triacetate foam targets preheated by radiation from a laser generated hohlraum and irradiated by an intense short pulse laser generated proton beam [9].

Alongside experiments reporting alpha particle yields from non-thermal p-B fusion, additional configurations were proposed, based on analytic, molecular dynamics, particle in cell and kinetic calculations. A design for table-top p-B fusion based on Coulomb explosion of hydrogen nanodroplets, irradiated by intense femtosecond laser pulse, contained in a solid boron cylinder was reported in [10]. A non-thermal laser-driven mixed fusion reactor concept based on nano-structures confined by electric and magnetic fields generated *in-situ* was suggested in [11]. A path to proton-boron fusion based on simulation of the interaction of a high energy attosecond pulse with a solid proton-boron target was proposed in [12]. A recent review of the challenges of non-thermal proton-boron fusion configurations was reported by [13].

Almost a decade ago, the possibility of increasing non-thermal p-B fusion reactivity in laser generated plasmas by energy transfer from the alpha particles to plasma protons was suggested [14]. It was claimed that this phenomenon, called also avalanche or chain reaction, could explain the high yield of alpha particles in an experiment at the PALS facility [2]. In the experiment in presented in [2], a yield of 10^8 alpha particles per pulse was obtained by irradiating a hydrogen-enriched boron-doped silicon target with a 500 J, 0.3 ns laser pulse. The avalanche mechanism has been a subject of debate. After criticism from [15, 16], the possibility of enhancement of p-B fusion reactivity by energetic protons generated via alpha-proton elastic collision was further elaborated by [17–19] and [20, 21]. It was shown that this process is inhibited by thermalization of the energetic protons, and that, during the alpha particles slowing down, most of the alpha energy is transferred to the plasma electrons. Using a model based on binary collisions, [17] calculated an avalanche time longer than the time scale of the PALS experiment. Moreover, [8] generalized the model to densities several order of magnitudes higher than solid density and temperatures up to 100 keV. While [22] considered reducing the stopping power by injecting a MeV proton beam into a highly compressed quantum degenerated boron target.

Recently, alpha heating leading to self-sustained fusion at temperatures higher than tens of keV, however, lower than the characteristic temperature for thermal fusion, at low density proton-boron plasma, was shown in simulations by [23].

In this paper we explore the possibility of boosting the reactivity of non-thermal proton-boron fusion triggered by an external proton beam in a plasma at density of the order of solid density, and the critical density, characteristic to laser plasma interaction.

2 The model

In the framework of the pitcher-catcher scheme, we consider a proton beam generated by an intense laser pulse, typically through the TNSA mechanism, interacting with a proton-boron plasma. In the simulations, we assume that the protons' energy spectrum is a delta function. Calculations were also made for a broad energy spectrum, characteristic to TNSA, however, it was found that the main findings of the present model do not change. The fusion probability P_f for the reaction $p + B = 3\alpha$, during the stopping of one proton of the beam in the plasma is calculated by:

$$P_f(v_0) = \left(1 - \prod_{v_p}\left(1 - n_B \sigma_f \frac{v_p}{S.P}\Delta v_p\right)\right) \tag{1}$$

where n_B is the boron plasma number density, v_0 is the initial proton velocity, the cross section for fusion is σ_f, and the stopping power of the protons in the boron plasma is S.P. The term in the brackets inside the product denotes the probability that the proton does not participate in a fusion event within a velocity decrease of Δv_p. The stopping power of a projectile particle in a plasma is calculated by [24]:

$$\begin{aligned} S.P &= \frac{dv_\alpha}{dt} = -\sum_\beta \nu_s^{\alpha|\beta} v_\alpha \\ \nu_s^{\alpha|\beta} &= \left(1 + \frac{m_\alpha}{m_\beta}\right)\psi\left(x^{\alpha|\beta}\right)\nu_0^{\alpha|\beta} \\ \nu_0^{\alpha|\beta} &= \frac{4\pi e_\alpha^2 e_\beta^2 \lambda_{\alpha\beta} n_\beta}{m_\alpha^2 v_\alpha^3} \\ x^{\alpha|\beta} &= \frac{m_\beta v_\alpha^2}{2kT_\beta} \\ \psi(x) &= \frac{2}{\sqrt{\pi}}\int_0^x t^{1/2} e^{-t} dt \end{aligned} \tag{2}$$

Where α is the projectile particle (proton in the case of the external proton beam and thermalization of bulk protons, or alpha particles during their thermalization) and β is the medium, electrons, bulk protons, and boron ions in the plasma. The projectile and bulk plasma particles charges and masses are e_α, e_β, m_α, m_β, respectively. The Coulomb logarithm $\lambda_{\alpha\beta}$ is calculated as a function the density and temperature for each plasma specie and varies from 5 to 20 at the conditions considered here (see Supplementary Appendix). The main contribution to the stopping power is due to energy loss to the electrons due to their lower mass, which is detrimental to generation of energetic secondary protons. In this context, non-neutral plasma with $\gamma = \frac{n_e}{n_i} \ll 1$ is considered here as well, to reduce the loss of energy to the electrons during the protons slowing down in the proton boron bulk plasma. The increase in the number of fusion events in non-neutral plasma was considered recently [25].

The cross section for p-B fusion as function of the proton energy in the center of mass of the p-B system is given in Figure 1. The resonance of interest for the model considered here is the resonance at 675 keV with a width of 300 keV. In the calculations the cross section (CS) based on recent evaluation reported by Sikora [26] was used (the green line).

Figure 2A shows the primary fusion probability calculated from Equations 1, 2, as a function of the proton energy at plasma temperature and density for the cases considered in the following (see also Tables 1, 2), for $\frac{n_B}{n_p} = 0.2$, for neutral and non-neutral plasma with $\frac{n_e}{n_i} = 0.001$. It is seen that for non-neutral plasma and proton energies close to 20 MeV the fusion probability may approach $P_{f0} \approx 1$, i.e., each proton generates one fusion event, during its slowing down in the plasma. However, for proton energies lower than 1 MeV, the fusion probability is lower than 1% at high plasma non-neutrality and temperature. At both temperatures considered here the fusion probability increases

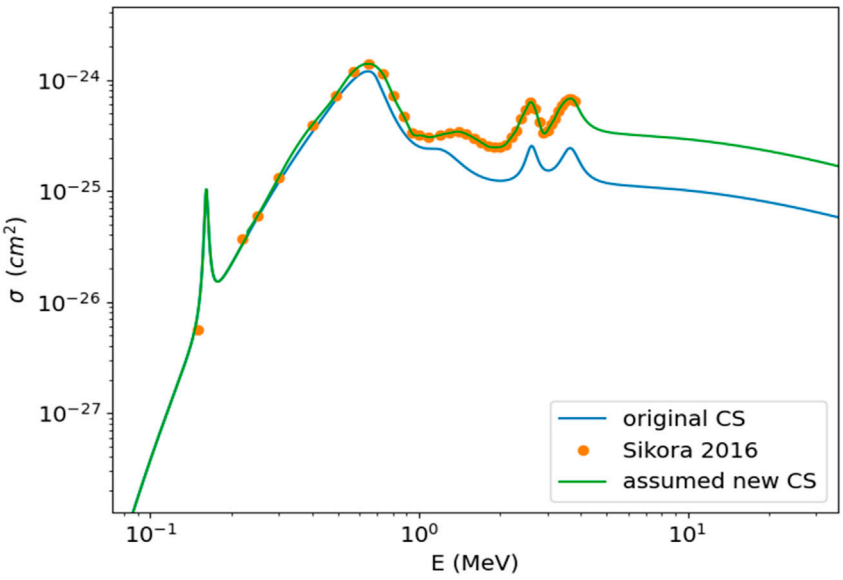

FIGURE 1
The cross section (CS) fusion probability as a function of the proton energy in the center of mass system based on analytical approximations of [27] original CS - blue, new evaluation from [26] - orange, the cross section used in the calculation presented here - green.

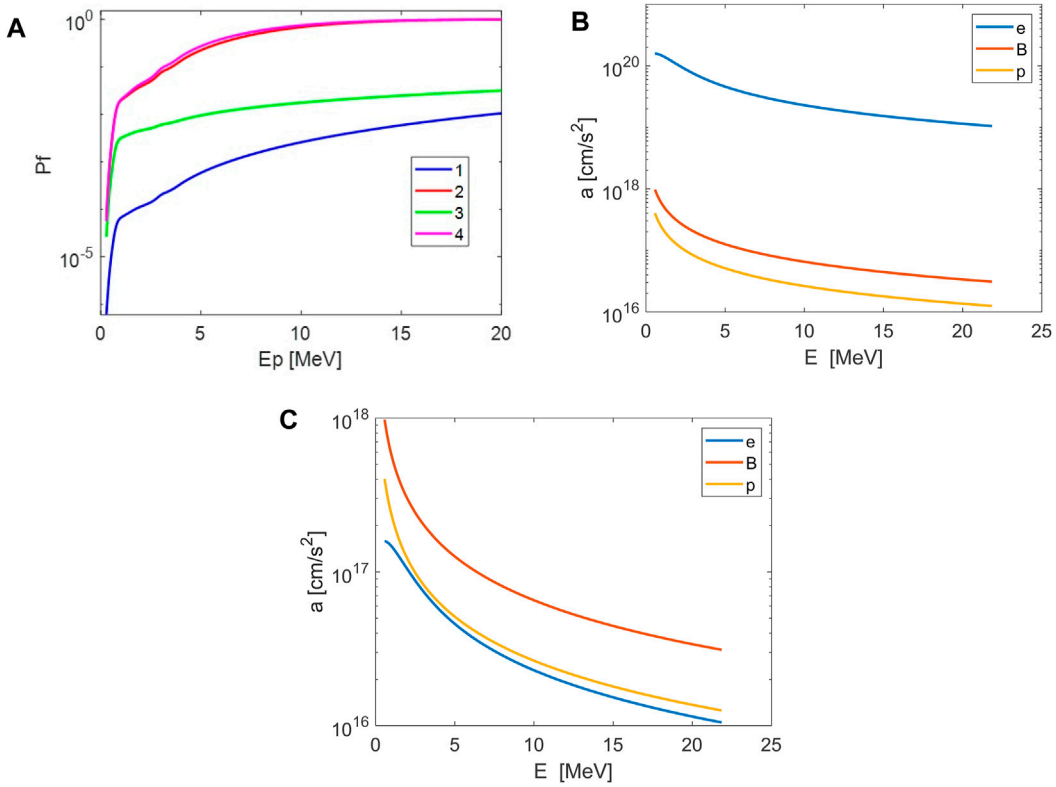

FIGURE 2
(A) The primary fusion probability as a function of the proton energy for neutral and non-neutral plasma with $\frac{n_{el}}{n_i}$ = 0.001, $\frac{n_B}{n_p}$ = 0.2. The graphs were calculated for electron and ion temperature and proton density: '1'- T_e = 340 eV, T_i = 100 eV and $n_p = 10^{23}$ cm^{-3} for neutral plasma; '2' - T_e, T_i and n_p are the same as in '1' but for non-neutral plasma, '3' - T_e = 10 keV, T_i = 1 keV and $n_p = 10^{21}$ cm^{-3} for neutral plasma; '4' - T_e, T_i and n_p are the same as in '3' but for non-neutral plasma. **(B)**: Electrons, protons and boron atoms contribution to the stopping power as a function of the proton beam energy for plasma conditions T_e = 340 eV, T_i = 100 eV, $n_p = 10^{23}$ cm^{-3}, neutral plasma, $\frac{n_B}{n_p}$ = 0.2 **(C)**: Electrons, protons and boron atoms contribution to the stopping power as a function of the proton beam energy for non-neutral plasma conditions T_e = 340 eV, T_i = 100 eV, $n_p = 10^{23}$ cm^{-3}, $\frac{n_e}{n_i}$ = 0.001 $\frac{n_B}{n_p}$ = 0.2.

TABLE 1 Plasma parameters used for solving Equations 3 at density n_p = 10^{23} cm^{-3} and temperature T_e = 340 eV, T_i = 100 eV.

	N_{p2}	N_{p3}	k_r (s^{-1})	τ_α (s)	τ_p (s)
Neutral plasma	0.4210^{-2}	0.310^{-2}	10^{11}	1.1710^{-11}	$4.24 \cdot 10^{-11}$
Non-neutral plasma	1.23	1.25	4.510^{9}	1.110^{-9}	710^{-9}

TABLE 2 Plasma parameters used for solving Equations 3 at density n_p = 10^{21} cm^{-3} and temperature T_e = 10 keV, T_i = 1 keV.

	N_{p2}	N_{p3}	k_r (s^{-1})	τ_α (s)	τ_p (s)
Neutral plasma	0.21	0.06	8.310^{7}	29.410^{-9}	56.610^{-9}
Non-neutral plasma	1.4	1.5	5.510^{7}	98.210^{-9}	62610^{-9}

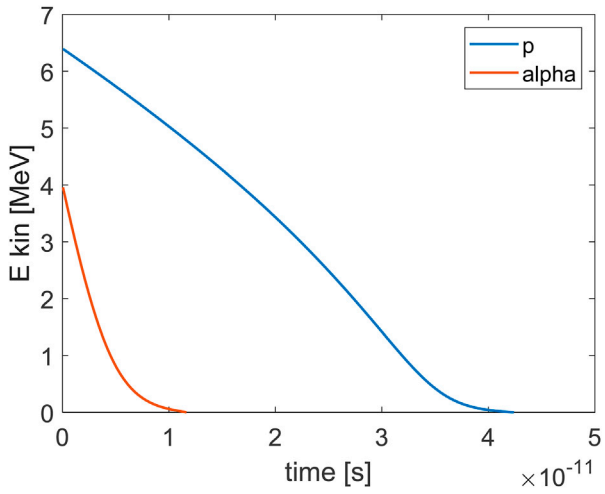

FIGURE 3
The kinetic energy of a proton beam with initial energy of 6.4 MeV and alpha particle with energy of 4 MeV, as a function of time during their slowing down in a proton-boron plasma with n_p = 10^{23} cm^{-3}, $\frac{n_B}{n_p}$ = 0.2, T_e = 340 eV, T_i = 100 eV, $\frac{n_e}{n_i}$ = 1.

with increasing temperature in neutral plasma and is less sensitive to temperature in non-neutral plasma, Figures 2B, C, display the electrons, protons and boron atoms contribution to the stopping power in neutral and non-neutral plasma at electron temperature 340 eV and proton density of 10^{23} cm^{-3}. In neutral plasma (Figure 2B) the stopping power is dominated by the electrons, while in non-neutral plasmas, this effect is mitigated (Figure 2C). The alpha particles generated in this primary fusion event may transfer energy by collisions to the bulk protons of the plasma, which may induce secondary fusion events. In addition, external beam protons that do not produce fusion may transfer energy to bulk protons in the plasma, which may as well contribute to secondary fusion events. An estimate of these secondary fusion events is calculated here.

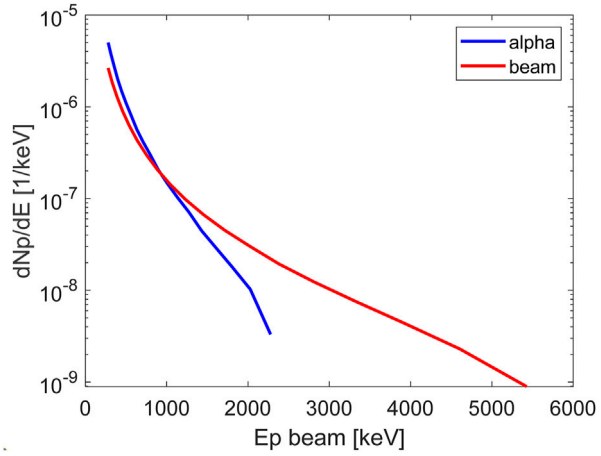

FIGURE 4
The energy spectrum of the secondary protons generated by an alpha particle with energy 4 MeV and a proton with energy 6.4 MeV during their slowing down to the ambient temperature in a proton-boron plasma with n_p = 10^{23} cm^{-3}, $\frac{n_B}{n_p}$ = 0.2, T_e = 340 eV, T_i = 100 eV, $\frac{n_e}{n_i}$ = 1.

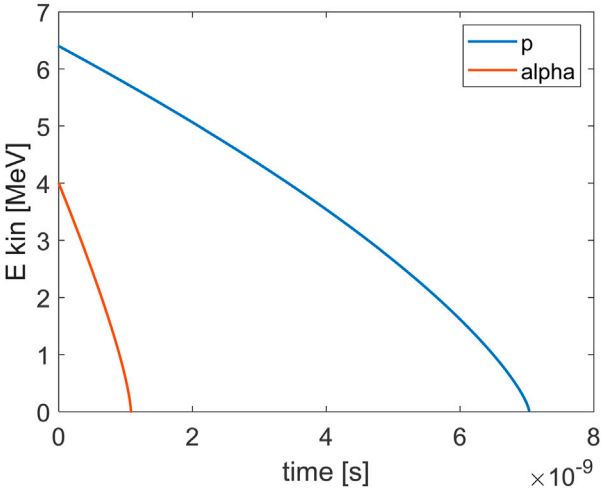

FIGURE 5
The kinetic energy of a proton beam with initial energy of 6.4 MeV and alpha particle with energy of 4 MeV, as a function of time during their slowing down in a proton-boron plasma with n_p = 10^{23} cm^{-3}, $\frac{n_B}{n_p}$ = 0.2, T_e = 340 eV, T_i = 100 eV, $\frac{n_e}{n_i}$ = 0.001.

Extending the model reported by Eliezer et al. [14] and Belloni et al. [17], the bulk protons number density is $n_p = n_{p1} + n_{p2} + n_{p3}$, where n_{p2} and n_{p3} denote the number density of the bulk protons which had useful collisions with an alpha particle and with a beam proton, respectively, getting energy to produce a secondary fusion event. It is assumed that this secondary fusion event occurs at cross section $\sigma_f = \sigma_{max}$, E = 675 keV. Assume that $n_{p2} \ll n_p$ and $n_{p3} \ll n_p$, i.e., the bulk proton density does not change.

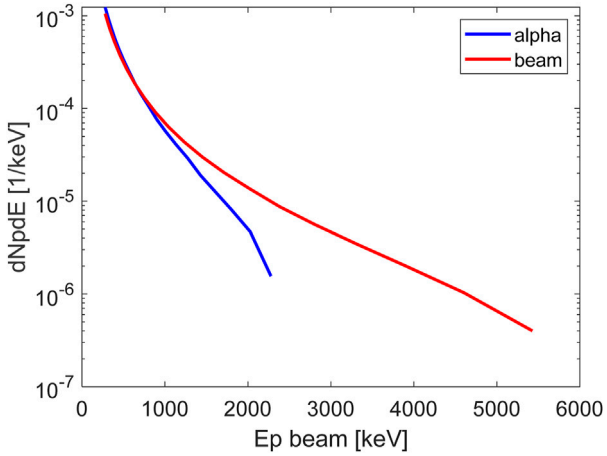

FIGURE 6
The energy spectrum of the secondary protons generated by an alpha particle with energy 4 MeV and a proton beam with energy 6.4 MeV during their slowing down to the ambient temperature in a proton-boron plasma with $n_p = 10^{23}$ cm^{-3}, $\frac{n_B}{n_p} = 0.2$, $T_e = 340$ eV, $T_i = 100$ eV, $\frac{n_e}{n_i} = 0.001$.

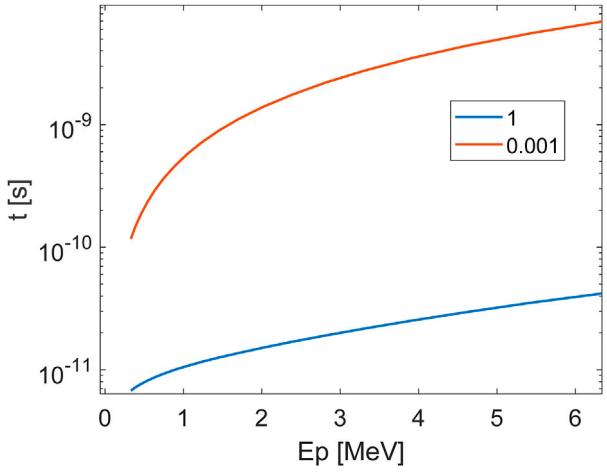

FIGURE 7
The relaxation time of the secondary protons as a function of energy in a proton-boron plasma with $n_p = 10^{23}$ cm^{-3}, $\frac{n_B}{n_p} = 0.2$, $T_e = 340$ eV, $T_i = 100$ eV, for neutral and non-neutral cases. The legend denotes the neutrality of the plasma, $\frac{n_e}{n_i}$.

The time dependent equations for the alpha particles and the energetic bulk protons number densities, n_α, n_{p2}, n_{p3} and the external proton beam velocity v_{pb} are:

$$\begin{aligned}
\frac{dn_\alpha}{dt} &= 3n_{pb} \cdot n_B \cdot \sigma_f v_{pb} + 3\left(n_{p2} + n_{p3}\right) n_B \sigma_{fmax} u \\
\frac{dn_{p2}}{dt} &= \frac{N_{p2} n_\alpha}{\tau_\alpha} - k_r n_{p2} - 3n_{p2} n_B \sigma_{fmax} u \\
\frac{dn_{p3}}{dt} &= \frac{N_{p3} n_{pb}}{\tau_b} - k_r n_{p3} - 3n_{p3} n_B \sigma_{fmax} u \\
\frac{dv_{pb}}{dt} &= SP
\end{aligned} \tag{3}$$

u is the velocity corresponding to the maximum value of the fusion cross section, SP is the stopping power defined in Equation 2, v_{pb} is the time dependent velocity of the beam protons in the plasma, n_{pb} is the effective number density of the proton beam, N_{p2} and N_{p3} denote the number of energetic protons generated by one alpha particle and one beam proton, respectively, during their slowing down and k_r is the relaxation rate of the energetic protons to the plasma temperature. The time dependent boron density is $n_B = n_B(t=0) - \frac{n_\alpha}{3}$. The stopping time of the alpha particles and the beam protons are τ_α and τ_b, respectively. N_{p2}, N_{p3} and k_r are calculated below.

In the calculations presented here $\varepsilon = \frac{n_B(t=0)}{n_p} = 0.2$. This value is beneficial for inducing secondary fusions, as it increases the probability of the generated alpha particle to collide with a light proton than with a heavier boron ion [18]. Bremsstrahlung radiation loss is not accounted for at the relatively low temperatures considered here, although we note that the above boron to proton density ratio is usually used in models describing thermal fusion.

The bulk proton-boron plasma is characterized by the electron and ion temperatures T_e and T_i , the proton, boron and electron number densities, n_p , n_B and n_{el}:

$$\begin{aligned}
n_B &= \varepsilon n_p \\
n_{el} &= \left(n_p + 5n_B\right)\gamma
\end{aligned} \tag{4}$$

where γ is the non-neutrality of the plasma. The number of energetic, secondary protons N_{p2} created by one alpha particle is estimated following Belloni [18]. The spectral distribution of the protons scattered during the slowing down of the alpha particle is:

$$\frac{dN_{p2}}{dE_{p2}} = n_p \int_{\frac{3}{2}T_i}^{E_\alpha} \sigma_s\left(E_\alpha, E_{p2}\right)\left(\frac{dE_\alpha}{dx}\right)^{-1} \frac{1}{E_{p2}} dE_\alpha \tag{5}$$

Where n_p is the number density of the bulk protons, E_p is the energy of the scattered proton, E_α is the energy of the alpha particle. Similarly, $\frac{dN_{p3}}{dE_{p3}}$ is the spectral distribution of secondary protons generated by the proton beam.

In our calculations, the cross section for the coulomb scattering, σ_s, is taken to be the Rutherford cross section:

$$\sigma_R = \frac{\pi}{E_\alpha E_p} \frac{\left(Z_\alpha Z_p e^2\right)^2 m_\alpha}{m_p} \tag{6}$$

The energy range of the scattered bulk protons is taken in the range (0.280 MeV - E_p^{max}), determined by a minimum energy for the "useful protons" considered by Shmatov [15] and Belloni et al. [17], and the maximum energy.

$$E_p{}^{max} = \frac{4m_\alpha m_p}{\left(m_\alpha + m_p\right)^2} E_\alpha \tag{7}$$

The number of protons N_{p2} generated by one alpha particle is obtained by integrating over the spectral distribution of the generated protons and is dependent on the plasma conditions.

In addition to Coulomb binary collisions, the nuclear contribution may increase the alpha particle–proton scattering cross section σ_S within a factor of 3 for $E_\alpha < 2$ MeV and up to a factor of 10 around $E_\alpha = 4$ MeV. For $E_\alpha > 4$ MeV and Ep < 1 MeV, $\frac{\sigma_S}{\sigma_R} < 1$ [18, 28]. To account for the sensitivity of the model presented here to the scattering cross section, the Equations 3

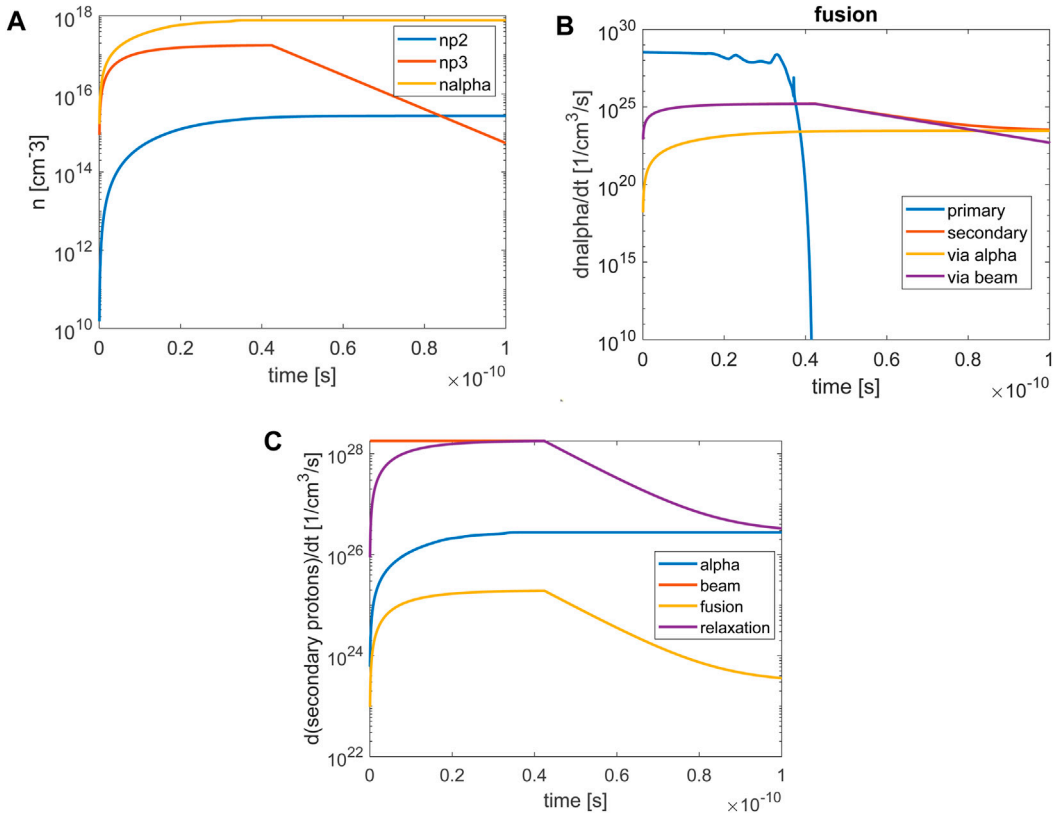

FIGURE 8
(A) The number density of alpha particles and secondary protons as a function of time, **(B)** the fusion reaction rate, **(C)** the source and sink terms for the secondary protons, as a function of time for neutral plasma and parameters in Table 1.

were solved also using a multiplier m for the Rutherford cross section, $\sigma_S = m\sigma_R$. For the plasma conditions considered here, the solution of Equations 3 shows that the number of secondary protons generated by the alpha particle N_{p2} increases linearly with the value of the multiplier.

The rate of relaxation k_r of the bulk energetic protons is calculated as the inverse of the stopping time of these protons averaged with their spectral distribution. The number of secondary energetic protons N_{p3} generated by the external beam proton is calculated similarly.

In the calculations, a monochromatic proton beam was used with energy of 6.4 MeV and effective beam proton density $n_{pb} = 10^{21}$ cm^{-3}. This value corresponds to an effective volume given by, $Vol = \pi R_L^2 v_{pb} \tau_L$ where the laser pulse spot radius and pulse duration are R_L and τ_L. Typical values in TNSA experiments are $R_L = 5\mu m$ and $\tau_L = 1ps$, which leads to the effective beam density shown above and a total number of about 10^{13} protons.

3 Results

In the following, the solution of the time dependent Equations 3 is shown for neutral and non-neutral plasma for two cases of proton-boron plasma. In all the calculations it is assumed that $\frac{n_B}{n_p} = 0.2$.

First, we assume near solid proton density of 10^{23} cm^{-3}, Te = 340 eV (the ionization energy of B^{4+} for an isolated atom [29]), Ti = 100 eV. These plasma parameters were chosen to extend the high density and degenerate plasma range considered by [18], to proton-boron fusion triggered by an external proton beam. The number of secondary protons generated by the alpha particles and the beam protons are calculated from Equations 5–7. At these plasma conditions for neutral plasma, the probability for a proton beam with energy of several MeV to produce one fusion event in neutral proton-boron plasma is less than 1%. The graphs in Figures 3–11 are calculated for beam proton energy of 6.4 MeV and alpha particle energy of 4 MeV, at the peak of the fusion generated alpha-particles energy spectrum. At this proton beam energy, plasma temperature and density, the probability for a proton to produce a fusion event is 0.001 in neutral plasma and 0.36 in non-neutral plasma with $\frac{n_e}{n_i} = 0.001$. Figure 3 shows the velocity of the proton beam and the alpha particle as a function of time, during their slowing down in the proton-boron plasma. The stopping time is tens of picoseconds at the high-density plasma. The energy spectrum of the secondary protons is shown in Figure 4. The energy spectrum of the secondary protons generated by the external beam extends to higher energies, however the energy spectrum of both groups of secondary protons favors lower proton energies. Figures 5, 6 show the slowing down and the energy spectrum of the secondary protons in the case of non-neutral plasma, $\frac{n_e}{n_i} = 0.001$, at the same density and temperature. One can see that in non-neutral plasma the stopping times are by two orders of magnitude longer, the energy spectrum scale is larger and the lower energies in the spectrum are

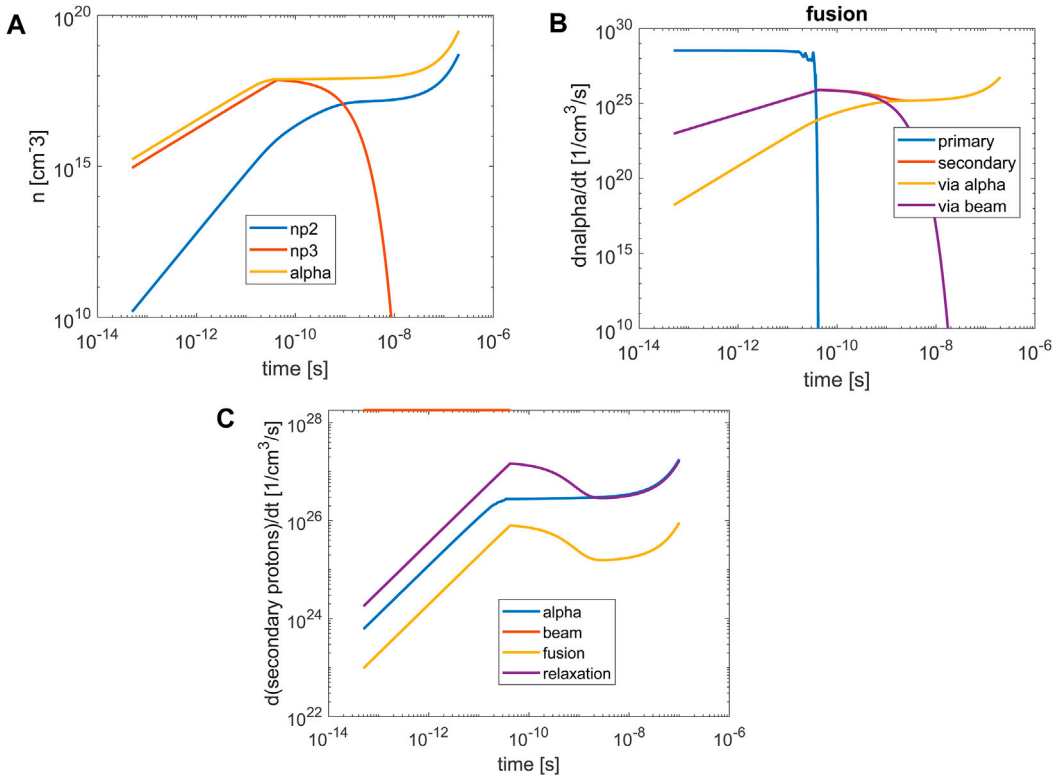

FIGURE 9
(A) The number density of alpha particles and secondary protons as a function of time, **(B)** The fusion reaction rate, **(C)** the source and sink terms for the secondary protons, as a function of time for neutral plasma and parameters in Table 1, with relaxation term for the secondary protons smaller by a factor of 50.

favorable, as for the case of neutral plasma. The relaxation times to ambient conditions of the secondary protons are shown in Figure 7. It is seen that the influence of the non-neutrality of the plasma on the relaxation times is larger at high energies, which are less favorable in the energy spectrum.

In Table 1 the plasma parameters used for solving the equations are given. N_{p2} is the number of secondary protons generated by one alpha particle with energy 4 MeV, calculated using the scattering cross section $\sigma_S = 5\sigma_R$. N_{p3} is the number of secondary protons generated by one beam proton with energy 6.4 MeV k_r is the relaxation rate of the secondary protons, obtained by averaging over the energy spectrum. The stopping time of the alpha and the beam protons are τ_α and τ_p, respectively.

In the following, a figure of merit describing boosting of reactivity by alpha generated secondary protons is defined by $\frac{n_{p2}}{n_p} \geq 0.01$. This ratio is consistent with the assumption of the model that the bulk proton density does not change.

The effective density of the proton beam in the calculations is $n_{pb} = 10^{21} cm^{-3}$.

Figures 8 displays the solution of Equations 3 for a neutral plasma. Figure 8A shows the number density of the alpha particles and secondary protons generated by the alpha and the external beam as a function of time, Figure 8B shows the fusion reactivity, while Figure 8C shows the terms relevant for the secondary fusion reaction rate. At early times the secondary protons are mainly generated by the external beam. As the beam slows down, these secondary protons decay. With onset of primary fusion secondary protons are generated by the alpha particles (Figure 8A). However, the fusion reaction rate generated by the secondary protons is about five orders of magnitude lower than the primary fusion (Figure 8B). An avalanche process does not occur, as it is mitigated by the secondary protons' relaxation term. The terms relevant for secondary fusion (Figure 8C) are:

$$source = \frac{N_{p2} n_\alpha}{\tau_\alpha} + \frac{N_{p3} n_{p3}}{\tau_{pb}} \tag{8}$$

$$fusion = 3\left(n_{p2} + n_{p3}\right) n_B \sigma_{fmax} u \tag{9}$$

$$relaxation = k_r\left(n_{p2} + n_{p3}\right) \tag{10}$$

The terms in Equations 8–10 are calculated and presented in Figures 8–10 for different plasma parameters. After the external beam slows down, the generation of secondary protons is balanced by their relaxation and secondary fusion is not boosted.

To illustrate the inhibition effect of the secondary fusion by the thermalization of the secondary protons, Equations 3 were solved for a lower relaxation term. Figures 9 shows the number density and the fusion reactivity, for a lower relaxation term by a factor of 50. After about 30 ns, the number density of the secondary protons increases, and secondary fusion is set. The confinement of the plasma to tens of nanoseconds might be achieved by magnetic

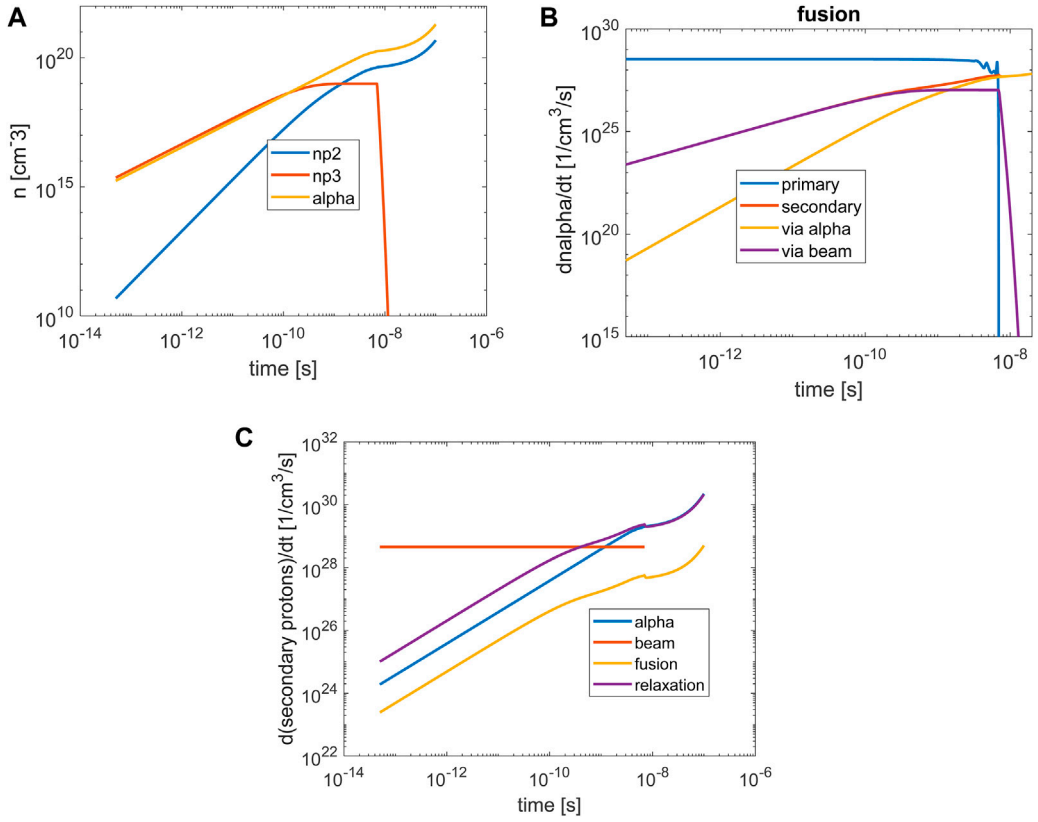

FIGURE 10
(A) The number density of alpha particles and secondary protons, **(B)** the rate of fusion events, as a function of time, for non-neutral plasma, **(C)** the number of secondary protons calculated with $\sigma_S = 5\sigma_R$ and relaxation rate in Table 1.

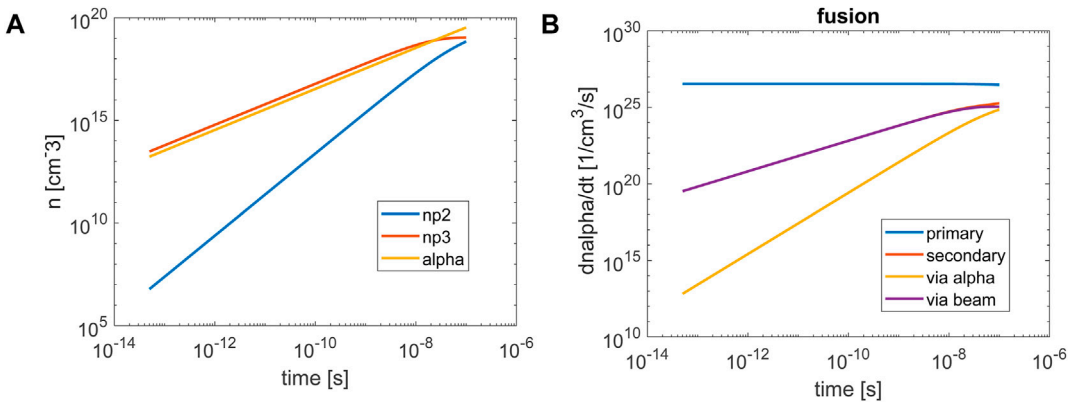

FIGURE 11
(A) The number density of the alpha particles and the secondary protons as a function of time for non-neutral plasma, density $n_p = 10^{21}$ cm^{-3} and temperature $T_e = 10$ keV, $T_i = 1$ keV, **(B)** the reaction rate of the fusion events. **(C)** the time dependence of the secondary protons.

fields, however, the possibility of decreasing the relaxation term is challenging.

Figure 10 displays the solution of Equations 3 for non-neutral plasma, with $\frac{n_e}{n_i} = 0.001$.

In this case, the number of secondary protons created by the alpha particles increases after the external beam slows down and the primary fusion stops (Figure 10A). The number of fusion events rises due to the secondary protons generated by the alpha particles. (Figure 10B). Figure 10C shows the terms that determine the time dependence of the secondary protons. The generation of the secondary protons due to the beam (red line) is constant and stops after the beam stops. The number of secondary protons generated by the alpha particles increases as the primary fusion develops and continues to increase after the beam stops, i.e., avalanche or boosting of fusion occurs (Figure 10C).

Secondly, we assume plasma parameters characteristic to laser plasma interaction, density $n_p = 10^{21}$ cm^{-3} and temperature T_e = 10 keV, T_i = 1 keV. The number of secondary protons and their relaxation time for neutral and non-neutral plasma are given in Table 2. Similarly to the high plasma density case, due to the large relaxation rate, the secondary protons do not induce secondary fusion in neutral plasma. Decreasing the relaxation rate by one order of magnitude, the secondary protons density reaches $\frac{n_{p2}}{n_p} = 0.01$ after 588 ns, and these secondary protons can induce secondary fusion events.

Figure 11 shows the number density of the alpha particles and the secondary protons for non-neutral plasma as a function of time for the plasma parameters shown in Table 2. The number densities of the alpha particles, secondary protons produced by the beam and by the alpha particles are shown in Figure 11A. It is seen that in this case the number of secondary protons reach $\frac{n_{p2}}{n_p} = 0.01$ after 130 ns, before the external proton beam stops. This ratio between the secondary and the bulk protons was chosen in the framework of the model as indicating onset of avalanche. Figure 11C shows the terms that determine the time dependence of the secondary protons.

4 Conclusion

The possibility of boosting non-thermal proton-boron fusion by energetic secondary protons generated by the alpha-particles through elastic scattering was investigated. Such a boosting may possibly lead to a self-sustained chain reaction. We consider proton-boron fusion induced by an external proton beam in a homogenous plasma of density and temperature of interest for laser driven experiments. The secondary protons energy spectrum and their thermalization was calculated, leading to three parameters, the effective number of secondary protons generated by an alpha particle and a beam proton during their slowing down and the relaxation rate of the secondary protons. With these three parameters, the possibility of secondary fusion was calculated, based on a simple three-population model. The results show that secondary fusion is inhibited by the fast thermalization of the secondary protons. The slowing down of the beam protons and the alpha particles in the bulk plasma were calculated using a stopping power based on Maxwellian distribution function for the particles in the plasma. In the framework of this model the charged particles transfer most of their energy to the electrons, inhibiting generation of suprathermal ions.

To decrease the effect of the thermalization of the secondary protons, non-neutral plasma was also considered in the calculation. In this case the relaxation rate of the secondary protons is much lower and secondary fusion occurs, leading to the desired avalanche effect.

Indeed, achieving such non-neutral plasma for fusion purposes is not trivial, however, such low electron density plasmas do occur, for example, in a double layer created at the interface of a laser-target interaction [30], or in a Debye sheath at a tokamak boundary [31].

Data availability statement

The raw data supporting the conclusions of this article will be made available by the authors, without undue reservation.

Author contributions

NN: Writing–original draft, Writing–review and editing, Conceptualization. ZH: Formal Analysis, Methodology, Software, Writing–original draft, Writing–review and editing. SE: Conceptualization, Writing–original draft, Writing–review and editing. YS: Methodology, Software, Writing–review and editing. CD: Writing–review and editing. SM: Formal Analysis, Writing–review and editing.

Funding

The author(s) declare that financial support was received for the research, authorship, and/or publication of this article. This work was supported by the Israeli Ministry of Energy and the Israeli Institute for Fusion Research.

Acknowledgments

We gratefully acknowledge the fruitful discussions with Fabio Belloni during the writing of this manuscript.

Conflict of interest

The authors declare that the research was conducted in the absence of any commercial or financial relationships that could be construed as a potential conflict of interest.

Publisher's note

Supplementary material

The Supplementary Material for this article can be found online at: https://www.frontiersin.org/articles/10.3389/fphy.2024.1428608/full#supplementary-material

References

1. Belyaev VS, Krainov VP, Matafonov AP, Zagreev BV. The new Possibility of the Fusion p + ^{11} B chain reaction being Induced by intense laser pulses. *Laser Phys Lett* (2015) 12:096001. doi:10.1088/1612-2011/12/9/096001

2. Picciotto A, Margarone D, Velyhan A, Bellutti P, Krasa J, Szydlowsky A, et al. Boron-proton nuclear-fusion enhancement induced in boron-doped silicon targets by low-contrast pulsed laser. *Phys Rev X* (2014) 4:031030. doi:10.1103/physrevx.4.031030

3. Margarone D, Picciotto A, Velyhan A, Krasa J, Kucharik M, Mangione A, et al. Advanced scheme for high-yield laser driven nuclear reactions. *Plasma Phys Control Fusion* (2015) 57:014030. doi:10.1088/0741-3335/57/1/014030

4. Giuffrida L, Belloni F, Margarone D, Petringa G, Milluzzo G, Scuderi V, et al. High-current stream of energetic α particles from laser-driven proton-boron fusion. *Phys Rev E* (2020) 101:013204. doi:10.1103/physreve.101.013204

5. Passoni M, Bertagna L, Zani A. Target normal sheath acceleration: theory, comparison with experiments and future perspectives. *New J Phys* (2010) 12:045012. doi:10.1088/1367-2630/12/4/045012

6. Labaune C, Baccou C, Depierreux S, Goyon C, Loisel G, Yahia V, et al. Fusion reactions initiated by laser-accelerated particle beams in a laser-produced plasma. *Nat Commun* (2013) 4:2506. doi:10.1038/ncomms3506

7. Baccou C, Depierreux S, Yahia V, Neuville C, Goyon C, De Angelis R, et al. New scheme to produce aneutronic fusion reactions by laser-accelerated ions. *Beams* (2015) 33:117–22. doi:10.1017/s0263034615000178

8. Bonvalet J, Nicolaï P, Raffestin D, D'humieres E, Batani D, Tikhonchuk V, et al. Energetic α -particle sources produced through proton-boron reactions by high-energy high-intensity laser beams. *Phys Rev E* (2021) 103:053202. doi:10.1103/physreve.103.053202

9. Zhao Y, et al. Proton-boron fusion: a dark horse in the fusion race shows yield much beyond expectation.

10. Last I, Ron S, Jortner J, Aneutronic H+ ^{B}11 nuclear fusion driven by coulomb explosion of hydrogen nanodroplets. *Phys Rev A* (2011) 83:043202. doi:10.1103/physreva.83.043202

11. Ruhl H, Korn G. A laser-driven mixed fuel nuclear fusion micro-reactor concept, (2022).

12. Ribeyre X, Capdessus R, Wheeler J, d'Humières E, Mourou G. Multiscale study of high energy attosecond pulse interaction with matter and application to proton–boron fusion. *Sci Rep* (2022) 12:4665. doi:10.1038/s41598-022-08433-4

13. McKenzie W, Batani D, Mehlhorn TA, Margarone D, Belloni F, Campbell EM, et al. HB11—understanding hydrogen-boron fusion as a new clean energy source. *J Fusion Energ* (2023) 42:17. doi:10.1007/s10894-023-00349-9

14. Eliezer S, Hora H, Korn G, Nissim N, Martinez Val JM. Avalanche proton-boron fusion based on elastic nuclear collisions. *Phys Plasmas* (2016) 23:050704. doi:10.1063/1.4950824

15. Shmatov ML. Comment on "avalanche proton-boron fusion based on elastic nuclear collisions" phys. Plasmas. *Phys Plasmas* (2016) 23:094703. doi:10.1063/1.4963006

16. Shmatov ML, Batani D. Analysis of the P- ^{11} B fusion Scenario with Compensation of the Transfer of kinetic Energy of Protons and alpha Particles to the gas Medium by the electric field, laser part. *Beams* (2022) 2022:e13. doi:10.1155/2022/7473118

17. Belloni F, Margarone D, Picciotto A, Schillaci F, Giuffrida L. On the enhancement of P-11B fusion reaction rate in laser-driven plasma by α → p collisional energy transfer. *Phys Plasmas* (2018) 25:020701. doi:10.1063/1.5007923

18. Belloni F. On a fusion chain Reaction via suprathermal Ions in high-density H– ^{11} B plasma. *Plasma Phys Control Fusion* (2021) 63:055020. doi:10.1088/1361-6587/abf255

19. Belloni F, Batani K. Multiplication Processes in high-density H- ^{11} B fusion fuel, laser part. *Beams* (2022) 2022:e11. doi:10.1155/2022/3952779

20. Ochs IE, Kolmes EJ, Mlodik ME, Rubin T, Fisch NJ. Improving the feasibility of economical proton-boron-11 fusion via alpha channeling with a hybrid fast and thermal proton scheme. *Phys Rev E* (2022) 106:055215. doi:10.1103/physreve.106.055215

21. Ochs IE, Fisch NJ. Lowering the reactor breakeven requirements for proton–boron 11 fusion. *Phys Plasmas* (2024) 31:012503. doi:10.1063/5.0184945

22. Liu SJ, Wu D, Hu TX, Liang TY, Ning XC, Liang JH, et al. Proton-boron fusion scheme taking into account the effects of target degeneracy. *Phys Rev Res* (2024) 6:013323. doi:10.1103/physrevresearch.6.013323

23. Moustaizis S, Daponta C, Eliezer S, Henis Z, Lalousis P, Nissim N, et al. Alpha heating and avalanche effect simulations for low density proton-boron fusion plasma. *J Inst* (2024) 19:C01015. doi:10.1088/1748-0221/19/01/c01015

24. Huba JD. *Beam Physics Branch, Plasma Physics Division*. Washington, DC: Naval Research Laboratory (2007): 20375.

25. Nissim N. Parametric scan of plasma parameters for optimization of the avalanche process in p_11B fusion. In: The 2nd international workshop on proton-boron fusion. Catania, Italy (2022).

26. Sikora MH, Weller HR. A New Evaluation of the 11B (p,α) α α Reaction Rates. *J Fusion Energ* (2016) 35:538–43. doi:10.1007/s10894-016-0069-y

27. Nevins WM, Swain R. The thermonuclear fusion rate Coefficient for P- ^{11} B reactions. *Nucl Fusion* (2000) 40:865–72. doi:10.1088/0029-5515/40/4/310

28. Gurbich AF. SigmaCalc recent development and present status of the evaluated cross-sections for IBA. *Nucl Instr Methods Phys Res Section B: Beam Interactions Mater Atoms* (2016) 371:27–32. doi:10.1016/j.nimb.2015.09.035

29. Lide DR. *CRC handbook of chemistry and physics: 2000-2001 a ready-reference book of chemical and physical data*. 81st ed. Boca Raton New York Washington: CRC Press (2000).

30. Eliezer S, Nissim N, Martínez Val JM, Mima K, Hora H. Double layer acceleration by laser radiation. *Laser Part Beams* (2014) 32:211–6. doi:10.1017/s0263034613001018

31. Vasileska I, Kos L. Time-dependent boundary conditions during ELMs in ITER plasma. *J Fusion Energ* (2020) 39:212–20. doi:10.1007/s10894-020-00241-w